의학박사 학위논문

Therapeutic co-targeting of WEE1 and ATM downregulates PD-L1 expression in pancreatic cancer

2019년 8월

서울대학교 대학원

의학과 내과학 전공

JIN MEIHUA

Therapeutic co-targeting of WEE1 and ATM downregulates PD-L1 expression in pancreatic cancer

지도교수 방영주

이 논문을 의학박사 학위논문으로 제출함

2019년 7월

서울대학교 대학원

의학과 내과학 전공

JIN MEIHUA

JIN MEIHUA의 석사학위논문을 인준함

2019년 7월

위 원 장 _____(인)

부위원장 _____(인)

위 원 _____(인)

위 원 _____(인)

위 원 _____(인)

Therapeutic co-targeting of WEE1 and ATM downregulates PD-L1 expression in pancreatic cancer

By

JIN MEIHUA

(Directed by Yung-Jue Bang, M.D., Ph.D.)

A Thesis Submitted in Partial Fulfillment of the Requirement
for the Degree of **Doctor of Science in Medicine**

Department of Internal Medicine College of Medicine
Seoul National University

July, 2019

Approved by Thesis Committee:

Professor _____ Chairman

Professor _____ vice chairman

Professor _____

Professor _____

Professor _____

ABSTRACT

Therapeutic co-targeting of WEE1 and ATM downregulates PD-L1 expression in pancreatic cancer

JIN MEIHUA

Department of Internal Medicine

Graduate School

College of Medicine

Seoul National University

Background: Pancreatic cancer (PC) is one of the most lethal cancers worldwide, but there are currently no effective targeted treatments. The DNA damage response (DDR) is under investigation for the development of novel anti-cancer drugs. Since DNA repair pathway alterations have been found frequently in PC, the purpose of this study was to test the DDR-targeting

strategy in PC using WEE1 and ATM inhibitors.

Materials and Methods: We performed *in vitro* experiments using a total of ten human PC cell lines to evaluate anti-tumor effect of AZD1775 (WEE1 inhibitor) alone or combination with AZD0156 (ATM inhibitor). We established Capan-1-mouse model for *in vivo* experiments to confirm our findings.

Results: In our research, we found that WEE1 inhibitor (AZD1775) as single agent showed anti-tumor effects in PC cells, however, targeting WEE1 upregulated p-ATM level. Here, we observed that co-targeting of WEE1 and ATM acted synergistically to reduce cell proliferation and migration, and to induce DNA damage *in vitro*. Notably, inhibition of WEE1 or WEE1/ATM downregulated PD-L1 expression by blocking GSK-3β serine 9 phosphorylation and decrease of CMTM6 expression. In Capan-1 mouse xenograft model, AZD1775 plus AZD0156 (ATM inhibitor) treatment reduced tumor growth and downregulated tumor expression of PD-L1, CMTM6, and CXCR2, all of which contribute to tumor immune evasion.

Conclusion: Dual blockade of WEE1 and ATM might be a potential therapeutic strategy for PC. Taken together, our results support further clinical development of DDR-targeting strategies for PC.

Keywords: Pancreatic cancer, DNA damage response, WEE1, ATM, PD-L1

Student Number: **2017-33939**

CONTENTS

LIST OF TABLES

LIST OF FIGURES

INTRODUCTION

Pancreatic cancer (PC) is one of the most lethal diseases worldwide, and there is an urgent need to develop effective therapies for this disease [1]. Recently, genomic analyses have revealed that many cancer susceptibility genes are frequently mutated in PC, including *KRAS* (92% of cases) and *TP53* (78%). In addition, germline and somatic mutations in genes encoding breast cancer 1 and 2 (*BRCA1*, *BRCA2*), ataxia telangiectasia mutated (*ATM*) and partner and localizer of BRCA2 (*PALB2*) are present in PC patients with frequencies of 5% (germline mutations) and 12% (somatic mutations) [1]. These genes play critical roles in the DNA damage response (DDR), which signals the presence of strand breaks and other forms of DNA damage and coordinates their repair. Paradoxically, mutations in genes that compromise the DDR can both cause and protect against cancer. On the one hand, defects in the DDR can lead to genomic instability and the accumulation of mutations that increase the probability of cancer. On the other hand, DDR pathway dysfunction can render tumor cells susceptible to chemotherapeutic agents that damage DNA and/or impair alternative DDR pathways [2]. Thus, targeting of specific molecules in the DDR is a potential strategy for the development of new drugs for cancers with urgent unmet needs, including PC.

The cellular response to DNA damage, including single-stranded or double-stranded DNA breaks, is controlled by a network of proteins that include damage-sensing proteins such as poly (ADP-ribose) polymerase (PARP);

transducers such as the kinases ataxia telangiectasia mutated (ATM) and ataxia telangiectasia and Rad3 related (ATR); and effectors such as the nuclear kinase WEE1, which is a key protein in cell cycle checkpoint control and inhibits entry into mitosis [2]. Ultimately, the DDR results in one of three outcomes for the cell: successful DNA repair, cell cycle arrest, or apoptosis.

Therapeutic targeting of the DDR pathway has been examined in diverse tumor types [2]. Notably, inhibition of PARP, ATM, ATR or WEE1 has been shown to abrogate DNA repair via homologous recombination (HR) in many cancers with a genetically defective DDR, thus leading to synthetic lethality [3-6]. WEE1 acts as a gatekeeper of the G2/M cell cycle checkpoint, and its activity increases during the S and G2 phases; thus, WEE1 inhibition can induce growth arrest in S phase [7]. In contrast, cancer cells expressing mutant *TP53* lack a functional G1 checkpoint, and DNA damage must be repaired during the G2/M transition. Given that *TP53* is often mutated in PC [7], PC is the good candidate for the development of the DNA damage response (DDR) acting agents.

The tumor microenvironment plays a critical role in cancer progression [8]. PC is unique compared with other tumor types in being surrounded by strong stroma. Abundant immunosuppressive cells reside in the tumor microenvironment, including regulatory T cells, myeloid-derived suppressor cells (MDSCs), M2-type macrophages, and cancer-associated fibroblasts (CAFs) [8, 9]. Recruitment of these cells establishes a barrier to the anti-tumor

immune response [8, 9]. In addition, signaling via the chemokine receptor CXCR2 can drive PC growth by recruiting MDSCs and tumor-associated neutrophils and by enhancing the metastatic process [9]. Programmed cell death ligand 1 (PD-L1) is a negative regulator of the immune response and acts by binding to its receptor programmed cell death 1 (PD-1) on T cells, which inactivates the cells and thus allows the tumor to escape immune surveillance [10]. Data from genomic analyses indicate that immunogenic subtype of PC, which exhibits high levels of PD-L1, cytotoxic T-lymphocyte-associated protein 4 (CTLA4) and CXCR2 among several subtypes [1]. Notably, the chemokine-like factor-like MARVEL transmembrane domain containing family member 6 (CMTM6) has been suggested as one of the mechanisms of regulation of PD-L1 through preventing PD-L1 degradation by lysosome [11].

Increasing evidence suggests the existence of crosstalk between the DDR signaling network and immune pathways [12, 13]. For example, recent studies have demonstrated that the DDR regulates PD-L1 expression in cancer cells via a pathway involving activation of STAT (signal transducer and activator of transcription) signaling and inactivation of glycogen synthase kinase-3β (GSK3β) [14, 15]. However, such interactions between the DDR and immune signaling have not yet been studied in PC.

Here, we evaluated the anti-tumor effects of targeting the DDR using a WEE1 inhibitor (AZD1775) and an ATM inhibitor (AZD0156) in PC cells *in vitro* and in a mouse xenograft model.

MATERIALS AND METHODS

1. Human cell lines and reagents

Ten human PC cell lines were employed in this study: Aspc-1, Capan-1, Capan-2, MIA PaCa-2, PANC-1, SNU213, SNU324, and SNU410 were purchased from the Korean Cell Line Bank (Seoul, Korea), and SNU2913 and SNU2918, patient-derived cell lines, were successfully established from patient. Cells were cultured in medium (MIA PaCa-2 and PANC-1 cells in DMEM, all other cell lines in RPMI-1640, both from Welgen Inc., Gyeongsan, Korea) supplemented with 10% fetal bovine serum and 10μg/mL gentamicin and were maintained at 37°C in a 5% CO_2 atmosphere. The WEE1 inhibitor AZD1775 and ATM inhibitor AZD0156 were kindly provided by AstraZeneca (Macclesfield, Cheshire, UK).

2. Cell viability assay

Cells were seeded in 96-well plates at a density of 2–8×10^3 cells per well, incubated overnight at 37°C, and then exposed to various concentrations of AZD1775 and/or AZD0156 for 3 days. No treatment was a control. A 50μL aliquot of 3-(4,5-dimethylthiazol-2yl)-2,5-diphenyltetrazolium bromide (MTT) solution (Sigma-Aldrich, St. Louis, MO, USA) was added to each well and the incubation was continued at 37°C for 4h. The medium was removed and 150μL of dimethyl sulfoxide (DMSO) was added to each well and mixed. The absorbance at 540nm was measured with a VersaMax Microplate Reader

(Molecular Devices, Sunnyvale, CA, USA). The experiments were performed three times.

3. Colony-forming assay

Cells ($0.5–4\times10^3$) were seeded in 6-well plates and exposed to various concentrations of AZD1775 for 10 days. The colonies were then stained with Coomassie Brilliant Blue for 2h and counted using Gel Doc system software (Bio-Rad, Hercules, CA, USA). Each experiment was repeated three times.

4. Western blot analysis

Cells (1×10^6) were seeded in 100-mm dishes and treated with AZD1775 and/or AZD0156 for 24, 72 or 120h. The cells were harvested and lysed in RIPA buffer containing protease inhibitors on ice for 30 min. Samples of lysate containing equal amounts of protein were resolved by SDS-PAGE and transferred to membranes for western blotting. Primary antibodies against the following molecules were purchased from Cell Signaling Technology (Beverley, MA, USA): ATR (#2790), p-ATR-Ser428 (#2853), caspase-7 (#9492), CDC2 (#9112), p-CDC2-Tyr15 (#9111), WEE1 (#4936), p-WEE1-Ser642 (#4910), c-Myc (#5605), p-NF-κB p65-Ser536 (#3033), NF-κB (#8242), MCL-1 (#4572), CtIP (#9201), MMP-9 (#3852), MMP-2 (#4022), PD-L1 (#13684), STAT-1 (#9172), and p-STAT-1-Tyr701 (#9167). Anti-β-actin antibody was from Sigma-Aldrich; antibodies against p-ATM-Ser1981 (#ab81292), ATM (#ab78), CXCR-2 (#ab217314), and PA32/RPA2 (#ab2175) were from Abcam Bioscience (Cambridge, UK); anti-p-RPA32 S4/S8 (#A300-

245A) was from Bethyl Laboratories (Montgomery, TX, USA); anti-γH2AX antibody (#05-636) was from Millipore (Billerica, MA, USA); anti-Rad51 (#sc-8349) and anti-glyceraldehyde 3-phosphate dehydrogenase (GAPDH; #sc-25778) were from Santa Cruz Biotechnology (Dallas, TX, USA); and anti-CMTM-6 (#PA5-34747) and secondary antibodies were from Thermo Fisher Scientific (Waltham, MA, USA).

5. Immunoprecipitation

Cells were seeded in 150 mm dishes at a density of 2.5×10^6 cells/dish, treated with inhibitors for 72h. Anti-PD-L1 antibody (#13684), anti-IgG antibody (#ab133470, Abcam Bioscience) and Protein A/G PLUS agarose (#sc-2003, Santa Cruz Biotechnology) were used. Finally, samples were analyzed by western blotting as described above.

6. Cell cycle analysis

Cells (2×10^5) were seeded in 60-mm dishes and treated with or without 1μM AZD1775 for 24h. The cells were then harvested, and fixed with 70% ethanol at −20°C for 2 days. An aliquot of 7μL of 20mg/mL RNase A (Invitrogen, Carlsbad, CA, USA) was added to each well and the plates were incubated for 10 min at 37°C. Finally, propidium iodide (PI; Sigma-Aldrich) was added to each well and the cells were analyzed on a FACSCalibur flow cytometer (BD Biosciences, Franklin Lakes, NJ, USA). Each experiment was repeated three times.

7. Annexin V/PI apoptosis assay

Cells (2×10^5) were seeded in 60-mm dishes and treated with or without 1μM AZD1775 for 48h. Apoptosis was measured by double-staining the cells with Annexin V-FITC and PI (#556547, BD Biosciences) according to the manufacturer's protocol. The cells were then analyzed on a FACSCalibur flow cytometer. Cells in early and late apoptosis were defined as Annexin V-FITC-positive/PI-negative and Annexin V-FITC-positive/PI-positive, respectively. The results are presented as the means of three independent experiments.

8. Comet assay

Cells (2×10^5) were treated with 1μM AZD1775 and/or AZD0156 for 24h, resuspended at 1×10^5 cells/mL in ice-cold phosphate-buffered saline (PBS), and mixed with molten LMAgarose at a ratio of 1:10. Aliquots were placed on comet slides and incubated at 4°C in the dark for 40 min. The slides were immersed in precooled lysis solution (#4250-050-01, Trevigen Inc., Maryland, USA) at 4°C for 40 min and then in freshly prepared alkaline unwinding solution (200mM NaOH, 1mM EDTA, pH >13) for 30 min at room temperature in the dark. The slides were subjected to electrophoresis for 30 min and dried at room temperature overnight. Diluted SYBR Green staining solution (100μL) was placed onto each circle of agarose and the samples were covered with a coverslip. Tail moment (migration of DNA fragments) and intensity (DNA content) were measured using the Comet Assay IV program (Andor Technology, Belfast, UK). Each condition was analyzed in three independent experiments.

9. Transwell migration assay

Migration assays were conducted using 6.5 mm Transwell insert chambers with 8 μm-pore polycarbonate membranes (#CLS3422, Sigma-Aldrich). Cells ($0.3–2×10^5$) were seeded into the upper chamber in 200μL medium containing 0.1% FBS, and 500μL medium containing 10% FBS was added to the lower chamber. AZD1775 and/or AZD0156 were added to the upper chamber and the plates were incubated at 37°C for 24h. The non-migrated cells remaining on the upper side of the membranes were removed with cotton swabs, and the filters were fixed with 4% paraformaldehyde (#P2031, Biosesang, Gyeonggi-do, Korea) for 20 min at room temperature. The membranes were then incubated in 1% crystal violet solution (#V5265, Sigma-Aldrich) for 10 min. The cell were visualized using microscope and photographed, and the cells were then dissolved by incubating the membranes in 300μL of 33% acetic acid (#1.00063.2511, Merck, Darmstadt, Germany) for 10 min. The liquid was collected and the absorbance at 573 nm was measured using a microplate reader.

10. PD-L1 expression analysis by flow cytometry

Cells ($2×10^5$) were seeded in 60-mm dishes and incubated with AZD1775 and/or AZD0156 for 72h. The adherent cells were harvested, resuspended in cell staining buffer (#420201, BioLegend, San Diego, CA, USA), and incubated with anti-PD-L1 antibody (#329708, BioLegend) for 30 min at room temperature. Cells were then washed once with the same buffer and analyzed on a FACSCalibur. The results are presented as the means of three independent

experiments.

11. Human cytokine array

Cells (1×10^6) were seeded in 60-mm dishes and exposed to AZD1775 and/or AZD0156 for 24h. The cell supernatant was then collected and 500μL/sample was analyzed using the Proteome Profiler Human Cytokine Array Kit (#ARY005B, R&D Systems, Minneapolis, MN, USA) according to the manufacturer's instructions. Spot intensities were measured using ImageJ software (National Institutes of Health, Bethesda, MD, USA).

12. Human phospho-kinase array

Cells (1×10^6) were seeded in 100-mm dishes and exposed to AZD1775 and/or AZD0156 for 72h. The cells were harvested, and lysate samples containing 300μg of proteins were analyzed using the Proteome Profiler Human Phospho-Kinase Array Kit (#ARY003B, R&D Systems) according to the manufacturer's instructions. Spot intensities measured using ImageJ software.

13. Tumor xenograft experiments

Animal experiments were performed at the Biomedical Center for Animal Resource Development of Seoul National University (Seoul, Korea) according to institutional guidelines, and prior approval of the study protocol was obtained from the Institutional Animal Care and Use Committee. Four-week-old female athymic nude mice were purchased from Orient Bio Inc. (Gyeonggi-do, South Korea). Capan-1 cells were resuspended at 3×10^7 cells in 100 μL of PBS and

injected subcutaneously. Tumor size was measured every other day and the volume was calculated using the formula: volume = [(width)^2 × height]/2. When the tumor volume reached 200 mm^3, the mice were randomly assigned to four groups of five mice to receive (1) vehicle (2-hydroxypropyl-β-cyclodextrin solution), (2) AZD1775 once daily at 30 mg/kg for 4 weeks (5 days on/2 days off), (3) AZD0156, as described for (2), or (4) AZD1775 plus AZD0156, as described for (2). All treatments were administered by oral gavage. Body weights and tumor sizes were measured every other day.

14. Mouse cytokine array

Immediately before sacrifice, the mice were bled and serum samples were prepared. Aliquots of 500μL were analyzed using the Proteome Profiler Mouse Cytokine Array Kit, Panel A (#ARY006, R&D Systems) according to the manufacturer's instructions. Spot intensities were measured using ImageJ software.

15. Statistical analysis

Analyses were conducted using SigmaPlot version 10.0 (Systat Software Inc., San Jose, CA, USA). Data are presented as the means ± standard errors (SE). All statistical tests were two-sided. Differences were considered significant if the p-values were <0.05. Half-maximal inhibitory concentrations (IC50) were calculated using SigmaPlot software. Combined drug effects were analyzed by calculating the combination index (CI) with CalcuSyn software (Biosoft, Cambridge, United Kingdom). CI values of <1, 1, and >1 indicate synergistic,

additive, and antagonistic effects, respectively.

RESULTS

1. WEE1 inhibition inhibits the proliferation of PC cells

To evaluate the anti-tumor effects of WEE1 inhibition in PC, we used the MTT assay to assess the proliferation of 10 human PC lines in the presence of AZD1775 for 72 h. As shown in Figure 1A, AZD1775 inhibited the proliferation of all PC cell lines in a dose-dependent manner. The concentrations causing 50% inhibition (IC50s) ranged from 0.5μM to 2.1μM (Table S1). To verify these data, we examined the ability of the PC cell lines to form colonies after 10 days of incubation with AZD1775. This analysis also indicated a profound suppression of colony formation in all PC cell lines (Fig. 1B), and the low IC50 values for colony formation (0.03–0.36μM) confirmed the sensitivity of human PC cells to WEE1 inhibition (Table S1). Because all 10 of the PC cell lines showed comparable inhibition by AZD1775, we randomly selected four cell lines (Capan-1, SNU213, SNU410, and SNU2913) for the following experiments.

To determine whether AZD1775 blocked signaling in the DDR pathway, we performed western blot analysis of the expression and activation (phosphorylation) of a number of molecules involved in DDR signaling downstream of WEE1. For these experiments, PC cells were incubated with or without AZD1775 for 24 h before analysis by western blotting. As shown in Figure 1C, we confirmed that AZD1775 dose-dependently reduced the expression of total and phosphorylated (p-) WEE1 in all PC cells tested. In

addition, AZD1775 also decreased the expression of phosphorylated cell division cycle protein 2 (p-CDC2), c-Myc, and phosphorylated nuclear factor kappa-light-chain-enhancer of activated B cells (p-NF κB), and upregulated the expression of γ-H2AX compared with control (Fig. 1C). These results suggest that AZD1775 monotherapy has anti-proliferative activity in PC cells.

2. WEE1 inhibition induces S-phase arrest and apoptosis in PC cells.

Since WEE1 inhibition reduced PC cell proliferation, we next determined whether AZD1775 induced apoptosis. For this, the cells were incubated with or without AZD1775 for 48 h and apoptosis was examined by flow cytometry of Annexin V/PI-stained cells or by western blot analysis of an apoptosis regulator, MCL-1, and an effector, cleaved caspase 7. We found that AZD1775 treatment significantly increased the proportion of apoptotic cells compared with control cells (Fig. 1D and 1E) and concomitantly diminished the expression of MCL-1 and elevated the expression of cleaved caspase-7 (Fig. 1F). Since WEE1 functions as a regulator of cell cycle progression, we also assessed the proportion of cells in the cell cycle phases by flow cytometric analysis of PI-stained cells. As shown in Figure 1G, a significantly greater proportion of cells treated with AZD1775 than control was arrested in S-phase. To verify this, we examined expression of phosphorylated replication protein A 32 (p-RPA32), an S-phase marker that binds to single-stranded DNA. Indeed, AZD1775 treatment for 24 h resulted in increased phosphorylation of RPA32 at serine 4 and 8, indicating that WEE1 inhibition leads to replication stress (Fig. 1H).

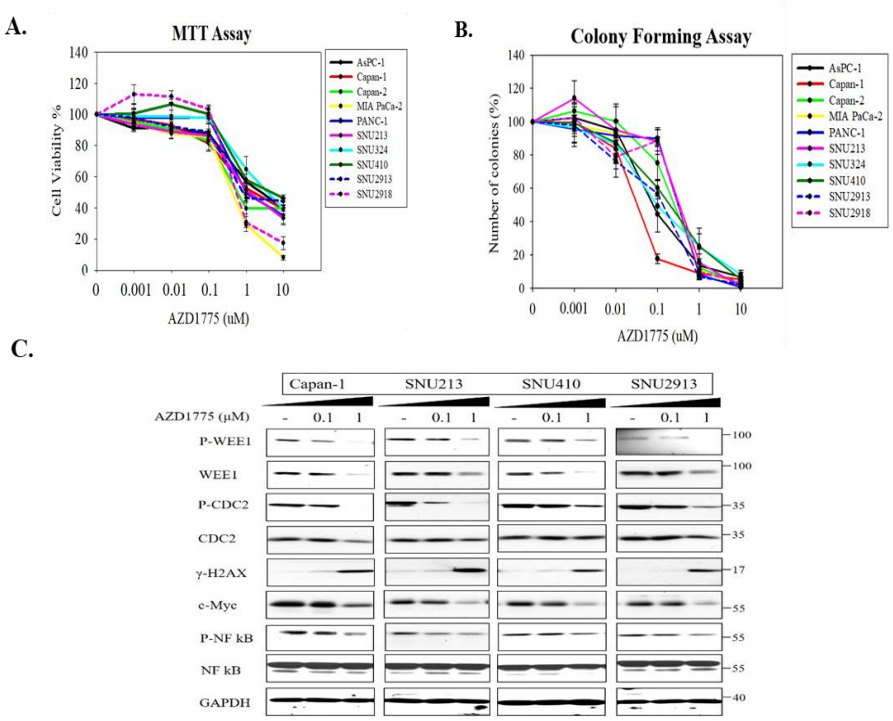

Figure 1. Growth inhibitory effect of AZD1775 in PC cell lines.

(**A**) Ten PC cell lines were exposed to control (0) or 0.001, 0.01, 0.1, 1, and 10μM AZD1775 for 72 h, and cell viability was measured using the MTT assay. (**B**) Cell lines were treated as described in (A) and colony formation was analyzed after 10 days. (**C**) Western blot analysis of total or phosphorylated signaling molecules in Capan-1, SNU213, SNU410, and SNU2913 cells treated with 0, 0.1 or 1μM AZD1775 for 24 h. Experiments were repeated three times.

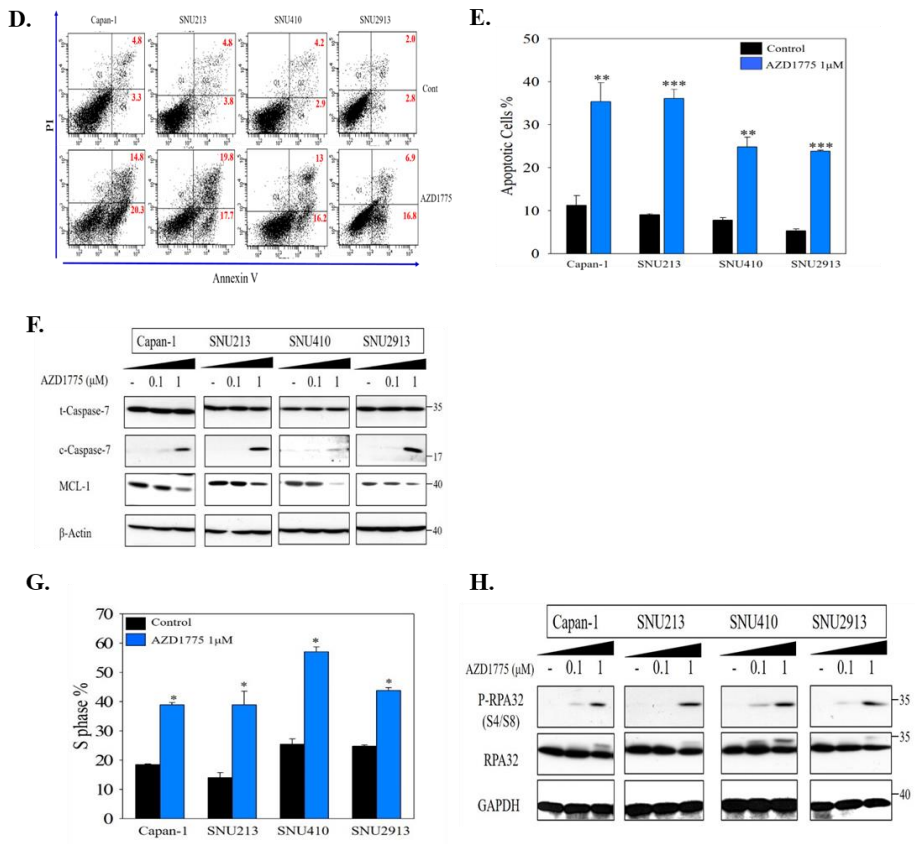

Figure 1. (**D**) Annexin V/PI apoptosis assay of Capan-1, SNU213, SNU410, and SNU2913 cells treated with 0 or 1μM AZD1775 for 48 h. (**E**) Quantification of three independent Annexin V/PI assays. **p*<0.05, ***p*<0.01, ****p*<0.001. (**F**) Western blot analysis of apoptosis-related proteins in cells treated with 0, 0.1, or 1μM AZD1775 for 48 h. (**G**) Cell cycle analysis of PI-stained PC cells treated with 0 or 1μM AZD1775 for 24 h. (**H**) Western blot analysis of cell cycle arrest-related signaling molecules in cells treated with 0, 0.1, or 1μM AZD1775 for 24 h. **p*<0.05, ***p*<0.01, ****p*<0.001. Experiments were repeated three times.

Table 1. MTT Assay and Colony Formation Assay IC50 of AZD1775 treatment.

Cell lines	AZD1775 (μM)	
	MTT	CFA
AsPC-1	1.6	0.08
Capan-1	1	0.03
Capan-2	0.6	0.25
MIA PaCa-2	0.5	0.3
PANC-1	1	0.3
SNU213	1	0.36
SNU324	2.1	0.1
SNU410	1.3	0.18
SNU2913	1.1	0.12
SNU2918	0.6	0.34

3. Co-inhibition of WEE1 and ATM profoundly impairs activation of the HR pathway of DNA repair

Having evaluated the effects of AZD1775 as a single agent, we asked whether WEE1 inhibition influences the activity of other core members of the DDR, such as ATM or ATR. Indeed, we found that phosphorylation of ATM and ATR was increased in cells treated for 24 h with AZD1775 (Fig. 2A). Since AZD1775 had a greater effect on promoting phosphorylation of ATM than of ATR, we next examined the anti-proliferative effects of AZD1775 in combination with the ATM inhibitor AZD0156 using the MTT assay. As shown in Figure 2B, the combination index (CI) values of AZD0156 plus AZD1775 were less than 1 for all four PC cell lines, indicating that the drugs had a synergistic effect on proliferation.

To better understand the effects of combination AZD1775 and AZD0156 treatment, we examined the expression levels of several molecules required for DNA repair via HR, after treatment of cells for 72h with AZD0156 and/or AZD1775. We found that expression of p-NF κB, Rad51, excision repair cross-complementing protein 1 (ERCC-1), C-terminal binding protein-interacting protein (CtIP), and p-STAT1 were all downregulated by AZD1775 or AZD0156 when added alone, but a greater effect was observed in cells co-treated with both agents (Fig. 2C). These data suggest that co-inhibition of WEE1 and ATM strongly blocks the HR pathway of DNA repair.

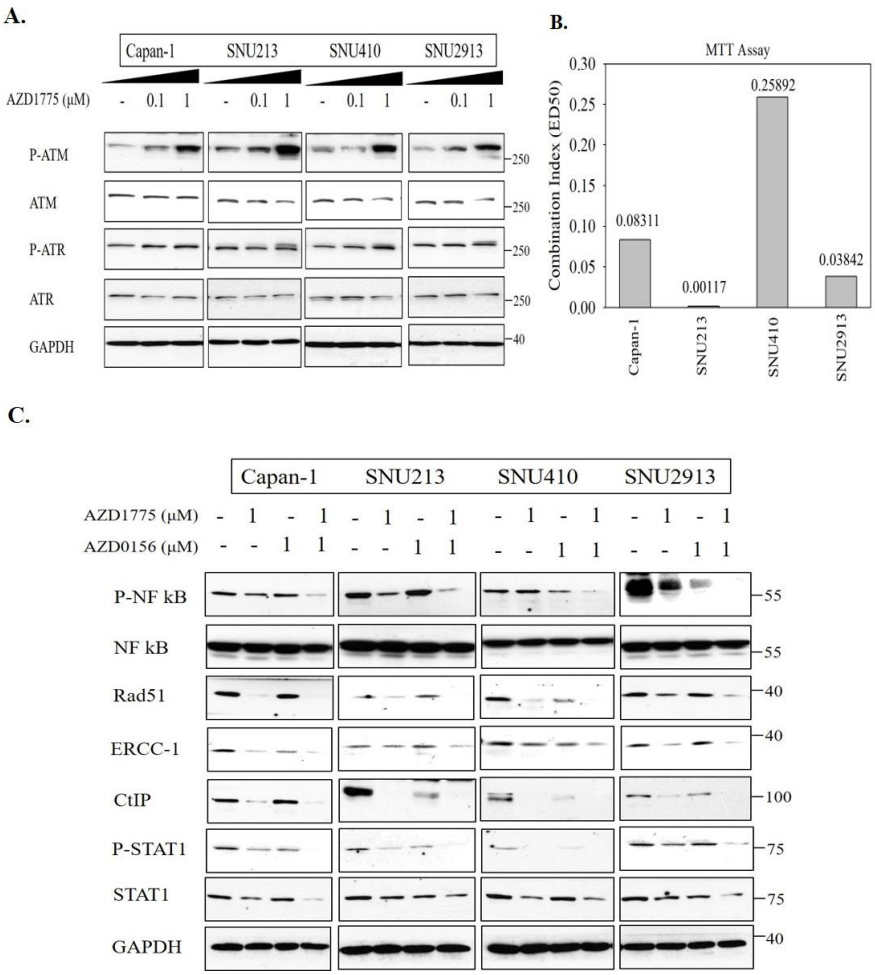

Figure 2. Effects of combination treatment with WEE1 and ATM inhibitors on cell growth.

(**A**) Western blot analysis of total and phosphorylated ATM and ATR in cells treated with 0, 0.1, or 1μM AZD1775 for 24 h. (**B**) CI values in the MTT assay after combination treatment with AZD1775 and AZD0156 for 72 h. CI >1, 1, <1 indicate antagonistic, additive, and synergistic effects, respectively. (**C**) Western blot analysis of cells treated with 0 or 1μM AZD1775 and/or AZD0156 for 72 h.

4. Co-inhibition of WEE1 and ATM synergistically induces DNA damage

Having demonstrated that co-inhibition of WEE1 and ATM blocks DNA repair, we next asked whether these agents could induce DNA damage. We exposed the cells to AZD1775 and/or AZD0156 for 24 h, and then monitored DNA fragmentation at the single-cell level using a comet assay. We found that AZD1775 or AZD0156 alone promoted DNA damage compared with control, but both agents in combination caused markedly increased fragmentation, as indicated by comet tail intensity and moment (Fig. 3A and 3B). Consistent with this, western blot analysis revealed upregulated expression of the DNA damage marker γ-H2AX, with a greater effect observed in cells subjected to combination AZD1775 and AZD0156 treatment compared with monotherapy (Fig. 3C).

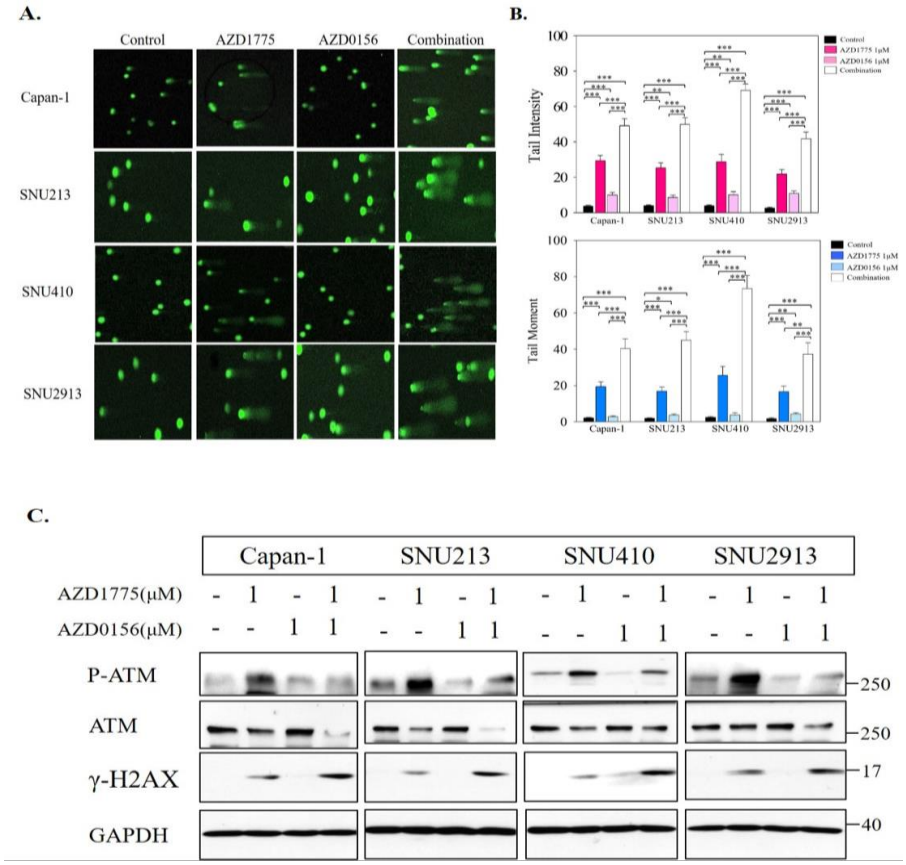

Figure 3. Effect of WEE1 and ATM co-inhibition on DNA damage.

(**A**) and (**B**) Displayed Comet Assay results after treated with 0, AZD1775 (1μmol/L) alone, AZD0156 (1μmol/L) alone, or both for 24 hours. Tail intensity and moment were analyzed using the Comet Assay IV program. (**C**) The related DNA damage signals were detected after exposed at combination treatment setting for 24 hours. *p<0.05, **p<0.01, ***p<0.001. Experiments were repeated three times.

5. Co-inhibition of WEE1 and ATM efficiently suppresses PC cell migration

To determine the consequences of WEE1 and ATM inhibition on PC cell function, we examined cell migration and invasion, which play well-characterized roles in cancer progression. Importantly, very few studies have evaluated the effects of DDR-targeted agents on tumor cell migration. In this study, Transwell migration assay was employed. Interestingly, we found that cell migration and invasion of all four PC cell lines were significantly suppressed by treatment with 1μM AZD1775 or AZD0156 alone. However, the combination of both drugs resulted in efficiently inhibition of cell migration (Fig. 4A and 4B). Thus, WEE1 and ATM appear to have previously unrecognized functions in promoting PC cell migration.

The matrix metallopeptidases 9 and 2 (MMP-9 and MMP-2) are known to be crucial for cancer metastasis and invasion [16, 17]. Therefore, we asked whether the effects of WEE1 and/or ATM inhibition on PC cell migration were mediated via these enzymes. Western blot analysis revealed that treatment with AZD1775 or AZD0156 for 24 h slightly decreased the expression of the smaller, active form of MMP-9 compared with control cells, and this effect was augmented by co-treatment with both agents (Fig. 4C). In contrast, a reduction in active MMP-2 expression was only observed in combination-treated Capan-1 and SNU410 cells (Fig. 4C).

Next, we investigated the effects of DDR targeting on chemokine expression

in Capan-1 cells using a human cytokine/chemokine array. We found that the chemokines interleukin 8 (IL-8), CXCL1, CCL5, and CCL2 were significantly downregulated by AZD1775 treatment, combination therapy again showed an enhanced inhibitory effect on all four chemokines (Fig. 4D and 4E). Interestingly, previous work showed that signaling via the receptors for these chemokines (CXCR2, CCR5, and CCR2), facilitate the release of MMP-9, which contributes to enhanced angiogenesis and tumor metastasis [18-20]. Collectively, our results suggest that AZD1775 and AZD0156 act synergistically to suppress PC cell migration by reducing chemokine expression and MMP-9 release.

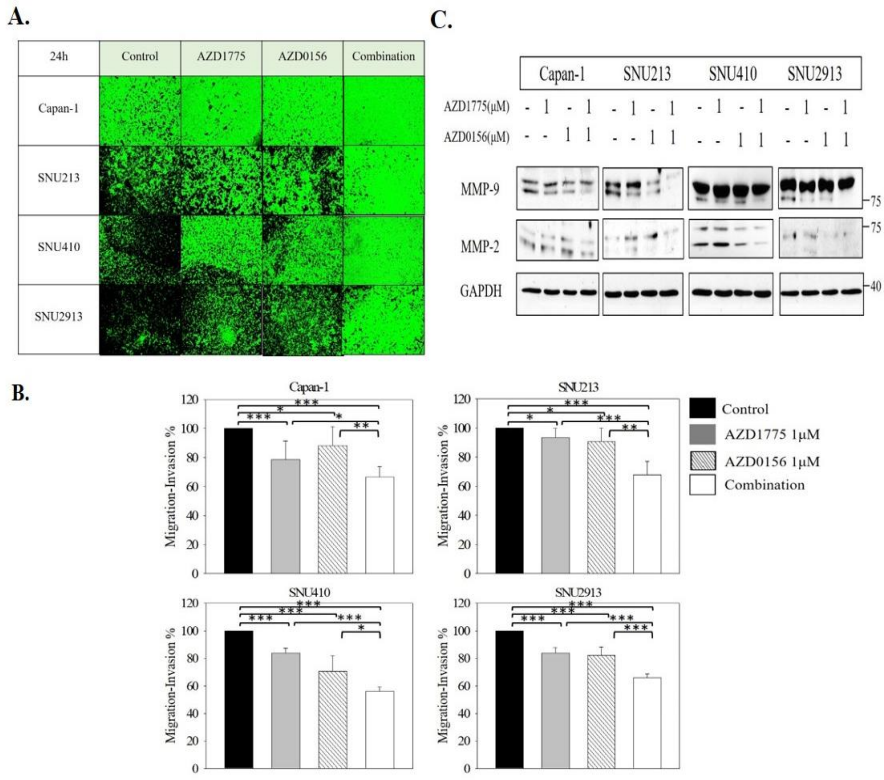

Figure 4. Effect of WEE1 and ATM co-inhibition on migration of PC cells.

(**A**) The anti-migration effect was evaluated using cells with 0, AZD1775 1μmol/L, or AZD0156 1μmol/L or both. The image was captured at 24 hours after treatment. (**B**) The percentage of migratory cells was analyzed after image was captured. The data represents three independent times. (**C**) Western blot analysis of migration-related molecules in cells treated as described in (A) for 24 h.

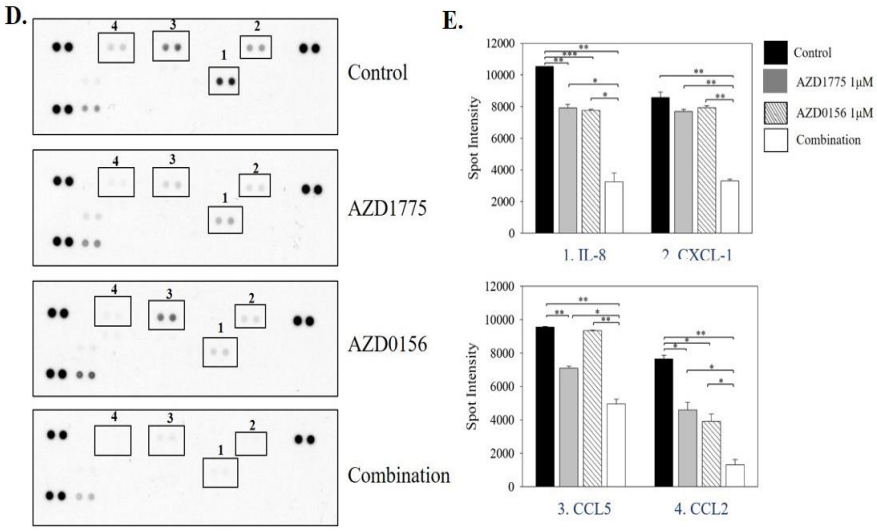

Figure 4. (**D**) and (**E**) Human cytokine array analysis of Capan-1 cells treated as described for (A) for 24 h. Spot intensities were quantified using ImageJ software. **1**, IL-8; **2**, CXCL-1; **3**, CCL5; **4**, CCL2. **p*<0.05, ***p*<0.01, ****p*<0.001.

6. Co-inhibition of WEE1 and ATM downregulates PD-L1 expression in PC cells

Next, given that the pivotal status of PD-L1 expression in cancer cell or cancer microenvironment [21], we explored the potential interaction between the DDR and the anti-tumor immune response by examining the effects of DDR-targeted agents on total and cell surface expression of PD-L1 in PC cells. Western blot analysis revealed that total cellular PD-L1 expression was decreased by AZD1775 or AZD0156 treatment alone, but combination treatment was even more effective (Fig. 5A). This pattern was also observed when cell surface PD-L1 expression was examined by flow cytometry, particularly in SNU2913 cells, which express high PD-L1 levels (Fig. 5B).

To understand in more detail the effects of WEE1 and ATM inhibition on PD-L1 expression, we investigated potential mechanisms that regulate PD-L1: CMTM6, which is thought to prevent PD-L1 degradation by lysosomes [11], and GSK-3β, which has recently been identified as a novel regulator of PD-L1 expression [22]. Western blot analysis of CMTM6 expression showed a marked decrease in the protein levels after treatment for 72 h with AZD1775 and AZD0156, either alone or in combination (Fig. 5A). We also observed the reduction of PD-L1 expression at 24 h and 120 h by AZD1775, AZD0156 and combination treatment (Fig. 5A). To probe CMTM6-mediated regulation of PD-L1 further, we asked whether this molecule is associated intracellularly by immunoprecipitating with anti-PD-L1 and probing for the presence of CMTM6

in the immunoprecipitates. We found that CMTM6 was present in western blots of anti-PD-L1 immunoprecipitates, but not control IgG immunoprecipitates, of all four PC cell lines (Fig. 5C). Notably, IP with anti-PD-L1 antibody showed the CMTM6–PD-L1 binding was decreased upon WEE1 or ATM inhibition, with the greatest effects observed upon dual inhibition (Fig. 5C). It is possible that the reduction of CMTM6 by AZD1775 and AZD0156 led to decrease of CMTM6-PD-L1 bound form, which ultimately increase the PD-L1 degradation by lysosome supported by previous report [11].

To determine whether PD-L1 expression might be affected by the regulator GSK-3β in PC cells [22], we examined changes in phosphorylated kinase expression in AZD1775 and/or AZD0156-treated cells using a human phospho-kinase array. We observed that while AZD1775 and AZD0156 both downregulated p-GSK-3β expression, the combination treatment was more effective than either agent alone (Fig. 5D and 5E). This indicated that PD-L1 expression not only controlled by CMTM6 but also influenced by GSK-3β activity to a certain extent. Moreover, we found the same inhibitory effects on several other phospho-kinases, including p-cAMP response element-binding protein (p-CREB), p-Src, p-focal adhesion kinase (p-FAK), p-Yes, and p-P53 (Fig. 5D and 5E). Taken together, these results indicate that dual blockade of WEE1 and ATM may reduce PD-L1 expression by downregulating the expression of CMTM6, and inactive GSK-3β.

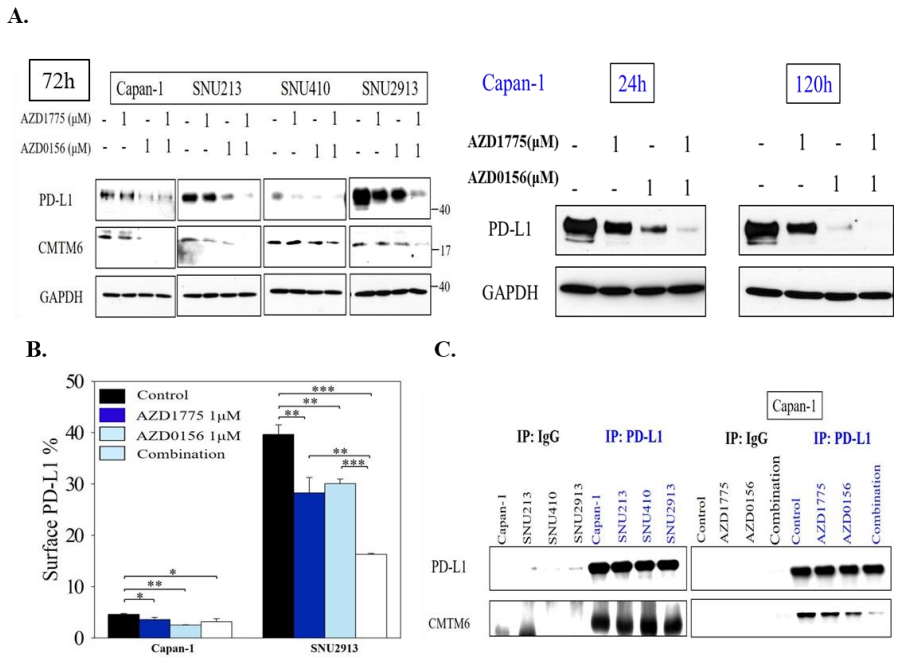

Figure 5. Effect of WEE1 and ATM co-inhibition on PD-L1 expression.

(**A**) Western blot analysis of PD-L1 and PD-L1-regulatory signaling molecules in PC cells treated with 0 or 1μM AZD1775 and/or AZD0156 for 72 h, 24h and 120 h. (**B**) FACS analysis of cell surface PD-L1 expression on Capan-1 and SNU2913 cells treated as described for (A) for 72 h. Experiments were repeated three times. (**C**) Western blot analysis of control IgG, or anti-PD-L1 immunoprecipitates treated as described for (A) for 72 h.

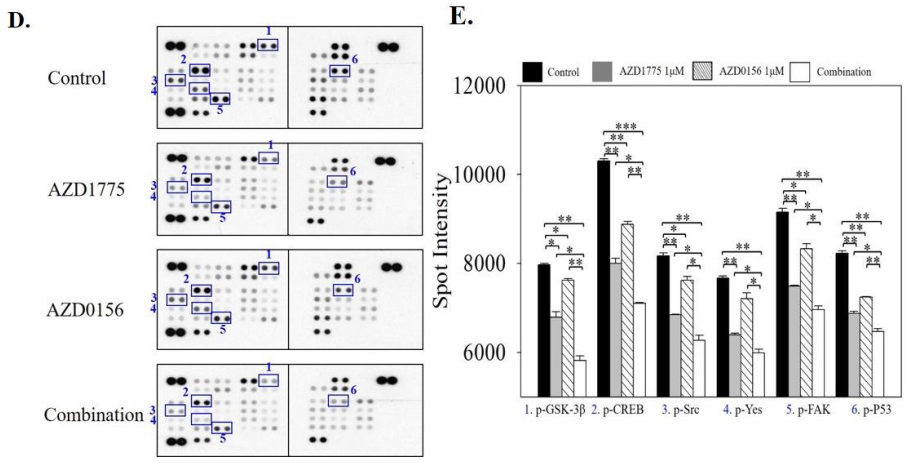

Figure 5. (**D**) and (**E**) Human phospho-kinase array analysis of Capan-1 cells treated as described for (A) for 24 h. Spot intensities were quantified using ImageJ software. **1**, GSK-3β Ser9; **2**, p-CREB Ser133; **3**, p-Src Tyr419; **4**, p-yes Tyr426; **5**, p-FAK Tyr397; **6**, p-P53 Ser15. *p<0.05, **p<0.01, ***p<0.001.

7. Co-inhibition of WEE1 and ATM augmented anti-tumor growth in Capan-1-xenograft model

To confirm the anti-tumor effect of AZD1775 and AZD0156 *in vivo*, Capan-1 xenograft model was established. Consistent with the *in vitro* observations, we found that single agent treatment with AZD1775 or AZD0156 significantly decreased tumor growth, but the combination treatment was markedly more effective than either agent alone ($p<0.05$; Fig. 6A). We observed no overt evidence of drug toxicity, as reflected by a lack of significant change in body weight (Fig. 6B).

Next, we excised the tumors and performed immunohistochemical (IHC) staining (Fig. 6C). Combination treatment with both drugs also potently inhibited staining of the proliferation marker Ki-67 and increased TUNEL staining, which detects fragmented DNA (Fig. 6C). In parallel, we performed western blot analysis to confirm our *in vitro* findings in the isolated tumors. In line with the in vitro results, we confirmed that AZD1775 treatment upregulated p-ATM while combination treatment with AZD1775 and the ATM inhibitor reversed this. Moreover, the expression of p-NF κB and CXCR2 were profoundly blocked by AZD1775 and/or AZD0156 treatment, and AZD1775 plus AZD0156 enhanced γ-H2AX accumulation. Furthermore, we validated the *in vitro* findings with PD-L1 and CMTM6 by confirming that both proteins were downregulated by single- or dual-agent treatment (Fig. 6D).

Finally, we assessed the effects of the DDR-targeting agents on immune cell

activity by analyzing cytokine levels in the sera of tumor-bearing mice. Using a mouse cytokine array, we found that release of C5a, TIMP metallopeptidase inhibitor 1 (TIMP-1), macrophage colony-stimulating factor (M-CSF), CD54, IL-16, and CXCL12 were markedly reduced by AZD1775 and/or AZD0156 treatment, with larger effects observed in drug combination-treated mice (Fig. 6E and 6F). Collectively, these *in vivo* data confirm that dual targeting of the DDR pathway components WEE1 and ATM profoundly suppress tumor growth *in vivo* compared with blockade of either molecule alone.

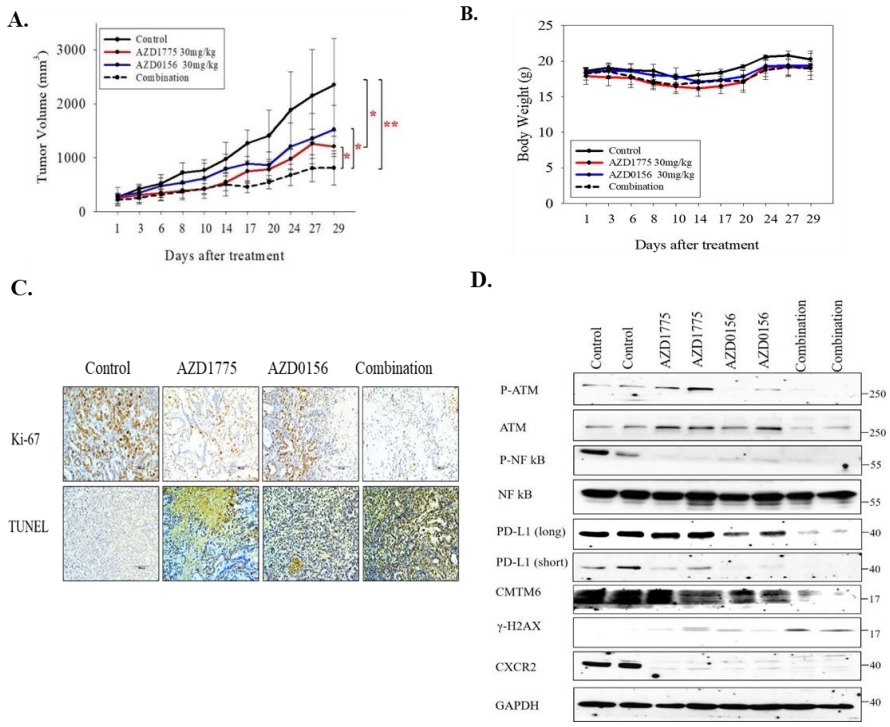

Figure 6. Anti-tumor effects of WEE1 and WEE1/ATM co-inhibition in the Capan-1 xenograft mouse model.

(**A**) and (**B**) Tumor growth curves (A) and mouse body weights (B) in Capan-1-xenografted mice treated with vehicle, AZD1775 (30 mg/kg), AZD0156 (30 mg/kg), or both AZD1775 and AZD0156 for up to 4 weeks. (**C**) Immunohistochemical analysis of Ki67, and TUNEL staining in Capan-1 xenografts excised tumors. Scale bars: 100 μm. (**D**) Western blot analysis of various proteins harvested from isolated tumors.

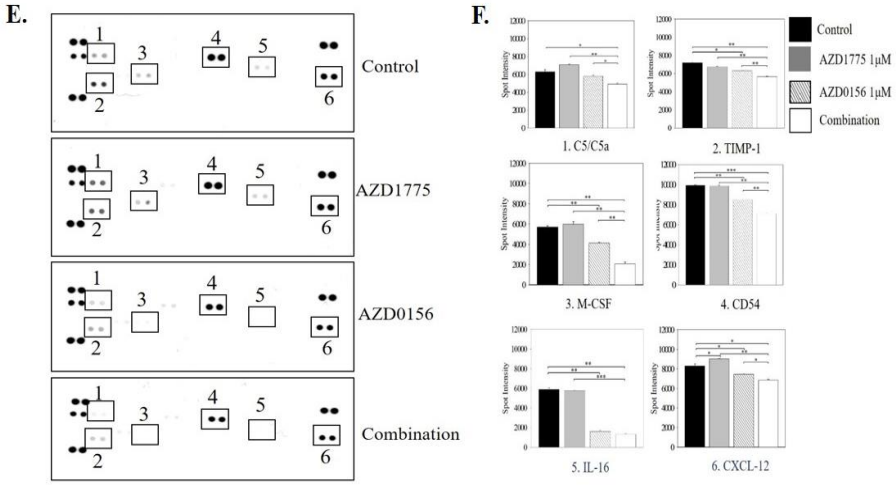

Figure 6. (**E**) and (**F**) Mouse cytokine array analysis of serum collected from xenografted mice. Spot intensities were measured using ImageJ software. **1**, C5/C5a; **2**, TIMP-1; **3**, M-CSF; **4**, CD54; **5**, IL-16; **6**, CXCL-12. *p<0.05, **p<0.01, ***p<0.001.

DISCUSSION

In this study, we demonstrate for the first time that targeting the DDR by inhibition of WEE1 has anti-tumor effects in PC and that co-inhibition of WEE1 and ATM amplifies these effects. We also evaluated the PD-L1 expression on cancer cells after treatment with WEE1 and ATM inhibitors.

One of the main findings of this study is that dual inhibition of WEE1 and ATM has profound effects on PC cell migration. Only a few studies have been performed on the anti-migratory effects of DDR-acting agents. One report showed that AZD1775 inhibits the migration of gastric cancer cells, although the mechanism of action was not elucidated [23]. Another study suggested that ATM might promote cell migration by regulating IL-8 expression independently of its role in DNA double-strand break repair [24]. We found that WEE1 and ATM co-inhibition reduced the expression of MMP-9, IL-8, CXCL1, CCL2, and CCL5, which is consistent with an anti-migratory effect. This is the first demonstration of the involvement of WEE1 or ATM in MMP-9 or IL-8 regulation. Moreover, downregulation of CXCR2, which is the IL-8 and CXCL1 receptor, in PC tumors was confirmed in our *in vivo* experiments. Although CXCR2 inhibition was shown to profoundly suppress metastasis and augments anti-PD-1 therapy in PC [9], the current study is the first to examine CXCR2 expression in PC. In addition, the involvement of Src and FAK in promoting cell migration and invasion is well known [25], and a recent report implicates a similar role for p-CREB [26]. Thus, our finding that expression of

p-CREB, p-Src, p-Yes, and p-FAK are profoundly inhibited by WEE1 and ATM co-inhibition is consistent with a role for these molecules in PC cell migration. Prior to this study, there had been no reports of a relationship between Src/FAK/CREB and the DDR pathway in PC.

An interesting recent study reported that PARP inhibition upregulates PD-L1 expression in breast cancer via inactivation of GSK-3β [15]. We also found a similar increase in PD-L1 expression in PARP inhibitor (Olaparib)-treated PC cells (data not shown). In contrast, the present study showed here that targeting of the DDR by WEE1 and/or ATM inhibition reduced PD-L1 expression concomitantly with downregulation of p-GSK-3β Ser9 level, the inactive form of GSK-3β. This mechanism might at least partly explain the reduction in PD-L1 induced by WEE1 and/or ATM inhibition. It is interesting to note that PARP, WEE1, and ATM have distinct effects on PD-L1 expression, despite the fact that they are all core members of the DDR signaling network. Thus, while PARP inhibition increases PD-L1 expression by enhancing GSK-3β inactivation, WEE1 and/or ATM inhibition does the opposite by decreasing the expression of inactive GSK-3β.

Among the mechanisms known to regulate PD-L1 expression, many act at the transcriptional level, including the JAK-STAT pathway, c-Myc, and NF-κB [14, 27, 28]. Consistent with this literature, we also observed a reduction in p-STAT-1 and p-NF κB concomitant with PD-L1 downregulation in WEE1 and/or ATM inhibitor-treated cells. More recently, Burr and colleagues used

CRISPR/Cas9 technology to screen approximately 20,000 genes in the human PC cell line BxPC-3, and they identified a novel protein, CMTM6, as a major regulator of PD-L1 expression [11]. Importantly, we observed that CMTM6 binds to PD-L1 in PC cells and that CMTM6 expression was reduced upon inhibition of WEE1 and/or ATM. The mechanism by which DDR targeting blocks CMTM6 expression remains to be clarified.

As we all known, both tumor and immune cells could express PD-L1 [21]. In our study, we focused on the PD-L1 expression in cancer cells by DDR-targeted agents. Whether the WEE1 or ATM inhibitors could regulate PD-L1 levels of immune cells, need to be further addressed. Most recently, intracellular PD-L1 has been demonstrated that participates DDR process and anti-PD-L1 treatment enhances cancer cells response to radiation or chemotherapy [29]. PD-L1 on cancer cells might have an important role of DDR signaling networks.

We used high concentrations of WEE1 inhibitor (AZD1775-1μM) and ATM inhibitor (AZD0156-1μM) in current in vitro experiments considering the active pharmacology of compounds. Particularly, AZD0156-1μM might have off-target effects.

Taken together, our results demonstrate that DDR-targeting agents such as WEE1 and ATM inhibitors have potent, synergistic anti-tumor effects in PC. WEE1/ATM inhibition downregulates CXCR2 and PD-L1 expression, the latter by blocking expression of inactive p-GSK-3β and CMTM6. The findings in this study support further clinical development of DDR-targeting strategies

for the treatment of PC.

REFERENCES

1. Bailey P, Chang DK, Nones K, Johns AL, Patch A-M, Gingras M-C, et al. Genomic analyses identify molecular subtypes of pancreatic cancer. Nature. 2016;531:47.

2. O'Connor MJ. Targeting the DNA Damage Response in Cancer. Mol Cell. 2015;60:547-60.

3. Richer AL, Cala JM, O'Brien K, Carson VM, Inge LJ, Whitsett TG. WEE1 Kinase Inhibitor AZD1775 Has Preclinical Efficacy in LKB1-Deficient Non-Small Cell Lung Cancer. Cancer Res. 2017;77:4663-72.

4. Kaufman B, Shapira-Frommer R, Schmutzler RK, Audeh MW, Friedlander M, Balmana J, et al. Olaparib monotherapy in patients with advanced cancer and a germline BRCA1/2 mutation. J Clin Oncol. 2015;33:244-50.

5. Chen CC, Kass EM, Yen WF, Ludwig T, Moynahan ME, Chaudhuri J, et al. ATM loss leads to synthetic lethality in BRCA1 BRCT mutant mice associated with exacerbated defects in homology-directed repair. Proc Natl Acad Sci U S A. 2017;114:7665-70.

6. Mohni KN, Kavanaugh GM, Cortez D. ATR pathway inhibition is synthetically lethal in cancer cells with ERCC1 deficiency. Cancer Res. 2014;74:2835-45.

7. Matheson CJ, Backos DS, Reigan P. Targeting WEE1 Kinase in Cancer. Trends Pharmacol Sci. 2016;37:872-81.

8. Binnewies M, Roberts EW, Kersten K, Chan V, Fearon DF, Merad M,

et al. Understanding the tumor immune microenvironment (TIME) for effective therapy. Nat Med. 2018;24:541-50.

9. Steele CW, Karim SA, Leach JDG, Bailey P, Upstill-Goddard R, Rishi L, et al. CXCR2 Inhibition Profoundly Suppresses Metastases and Augments Immunotherapy in Pancreatic Ductal Adenocarcinoma. Cancer Cell. 2016;29:832-45.

10. Chen DS, Mellman I. Oncology meets immunology: the cancer-immunity cycle. Immunity. 2013;39:1-10.

11. Burr ML, Sparbier CE, Chan YC, Williamson JC, Woods K, Beavis PA, et al. CMTM6 maintains the expression of PD-L1 and regulates anti-tumour immunity. Nature. 2017;549:101-5.

12. Chatzinikolaou G, Karakasilioti I, Garinis GA. DNA damage and innate immunity: links and trade-offs. Trends Immunol. 2014;35:429-35.

13. Rosado MM, Bennici E, Novelli F, Pioli C. Beyond DNA repair, the immunological role of PARP-1 and its siblings. Immunology. 2013;139:428-37.

14. Sato H, Niimi A, Yasuhara T, Permata TBM, Hagiwara Y, Isono M, et al. DNA double-strand break repair pathway regulates PD-L1 expression in cancer cells. Nat Commun. 2017;8:1751.

15. Jiao S, Xia W, Yamaguchi H, Wei Y, Chen MK, Hsu JM, et al. PARP Inhibitor Upregulates PD-L1 Expression and Enhances Cancer-Associated Immunosuppression. Clin Cancer Res. 2017;23:3711-20.

16. Farina AR, Mackay AR. Gelatinase B/MMP-9 in Tumour Pathogenesis and Progression. Cancers (Basel). 2014;6:240-96.

17. Gialeli C, Theocharis AD, Karamanos NK. Roles of matrix metalloproteinases in cancer progression and their pharmacological targeting. Febs j. 2011;278:16-27.

18. Zarogoulidis P, Katsikogianni F, Tsiouda T, Sakkas A, Katsikogiannis N, Zarogoulidis K. Interleukin-8 and interleukin-17 for cancer. Cancer Invest. 2014;32:197-205.

19. Chuang JY, Yang WH, Chen HT, Huang CY, Tan TW, Lin YT, et al. CCL5/CCR5 axis promotes the motility of human oral cancer cells. J Cell Physiol. 2009;220:418-26.

20. Tang CH, Tsai CC. CCL2 increases MMP-9 expression and cell motility in human chondrosarcoma cells via the Ras/Raf/MEK/ERK/NF-kappaB signaling pathway. Biochem Pharmacol. 2012;83:335-44.

21. Topalian SL, Drake CG, Pardoll DM. Immune checkpoint blockade: a common denominator approach to cancer therapy. Cancer Cell. 2015;27:450-61.

22. Li CW, Lim SO, Xia W, Lee HH, Chan LC, Kuo CW, et al. Glycosylation and stabilization of programmed death ligand-1 suppresses T-cell activity. Nat Commun. 2016;7:12632.

23. Chen D, Lin X, Gao J, Shen L, Li Z, Dong B, et al. Wee1 Inhibitor AZD1775 Combined with Cisplatin Potentiates Anticancer Activity against Gastric Cancer by Increasing DNA Damage and Cell Apoptosis. Biomed Res Int. 2018;2018:5813292.

24. Chen WT, Ebelt ND, Stracker TH, Xhemalce B, Van Den Berg CL,

Miller KM. ATM regulation of IL-8 links oxidative stress to cancer cell migration and invasion. Elife. 2015;4.

25. Kolli-Bouhafs K, Sick E, Noulet F, Gies JP, De Mey J, Ronde P. FAK competes for Src to promote migration against invasion in melanoma cells. Cell Death Dis. 2014;5:e1379.

26. Zhang ZX, Zhang WN, Sun YY, Li YH, Xu ZM, Fu WN. CREB promotes laryngeal cancer cell migration via MYCT1/NAT10 axis. Onco Targets Ther. 2018;11:1323-31.

27. Garcia-Diaz A, Shin DS, Moreno BH, Saco J, Escuin-Ordinas H, Rodriguez GA, et al. Interferon Receptor Signaling Pathways Regulating PD-L1 and PD-L2 Expression. Cell Rep. 2017;19:1189-201.

28. Asgarova A, Asgarov K, Godet Y, Peixoto P, Nadaradjane A, Boyer-Guittaut M, et al. PD-L1 expression is regulated by both DNA methylation and NF-kB during EMT signaling in non-small cell lung carcinoma. Oncoimmunology. 2018;7:e1423170.

29. Tu X, Qin B, Zhang Y, Zhang C, Kahila M, Nowsheen S, et al. PD-L1 (B7-H1) Competes with the RNA Exosome to Regulate the DNA Damage Response and Can Be Targeted to Sensitize to Radiation or Chemotherapy. Mol Cell. 2019.

국문 초록

췌장암은 전 세계적으로 가장 치명적인 암중의 하나이지만 현재 효과적인 표적치료제가 없다. 최근 DNA 손상 반응을 이용한 새로운 항암제 개발 연구가 큰 각광을 받고 있다. 췌장암에서 DNA 복구 경로의 변이가 많이 보고되어 있다. 이에 본 연구는 WEE1과 ATM 억제제를 이용하여 췌장암 세포주에서 DNA 손상 반응을 이용한 새로운 치료 전략을 연구하고자 진행되었다.

10개의 췌장암 세포주를 이용한 in vitro 실험을 통하여 AZD1775 (WEE1 억제제)의 단독 또는 AZD0156 (ATM 억제제)와의 병합 요법을 테스트 하였다. 이 결과를 바탕으로 Capan-1 마우스 모델에서 이 두가지 항암제의 항종양효과를 관찰하였다.

실험 결과 AZD1775는 단독 치료는 모든 췌장암 세포주들에서 효과적으로 세포 증식을 억제하고 s-phase의 증가와 세포사멸을 유도하는 등 뛰어난 항암효과를 보였고 반면에 p-ATM의 발현을 증가시켰다. AZD1775와 AZD0156의 병합 요법은 세포 증식과 전이를 억제하고 DNA 손상을 유도하는 방면에서 시너지 효과를 나타냈다. 또한 이런 병합 요법은 p-GSK 3β와 CMTM6의 발현을 감소시킴으로써 PD-L1의 발현을 현저히 감소시키는 것을 확인 하였다. In vivo 모델에서도 병합 요법은 종양의 성장을 억제할 뿐만 아니라 면역 반응에서 중요한 역할을 하는 PD-L1, CMTM6, CXCR2의 발현도 감소시킴을 확인 하였다.

이 연구의 결과는 WEE1와 ATM의 병용 요법의 항종양효과는 췌장암에서의 잠재적인 표적치료제가 될 수 있는 근거를 제시하고

더 나아가 임상에서 DNA 손상 반응을 표적으로 하는 치료제 개발 전략에 대한 근거를 제공한다.

주요어: 췌장암, DNA 손상 반응, WEE1, ATM, PD-L1

학번: 2017-33939